

1 **Hierarchizing multi-scale environmental effects on agricultural pest population dynamics: a case**
2 **study on the annual onset of *Bactrocera dorsalis* population growth in Senegalese orchards**

3
4
5 **Authors:** Cécile Caumette^{1,2,3}, Paterne Diatta⁴, Sylvain Piry¹, Marie-Pierre Chapuis^{1,2}, Emile Faye³,
6 Fabio Sigris⁵, Olivier Martin⁶, Julien Papaïx⁶, Thierry Brévault⁷, Karine Berthier⁸

7
8
9 **Addresses:**

10 ¹CBGP, Montpellier SupAgro, INRAE, IRD, CIRAD, University of Montpellier, Montpellier, France

11 ²CIRAD, CBGP, Montpellier, France

12 ³CIRAD, UPR Hortsys, F-34398, Montpellier, France

13 ⁴ISRA/CRA de Djibélor, Ziguinchor, Sénégal

14 ⁵Seminar for Statistics, ETH Zurich, Switzerland

15 ⁶INRAE, BioSP, 84914 Avignon, France

16 ⁷CIRAD, UPR AIDA, F-34398, Montpellier, France.

17 ⁸INRAE, Pathologie Végétale, F-84140, Montfavet, France

18

19

20 Corresponding author: cecile.caumette@cirad.fr

21 **ABSTRACT**

22 Implementing integrated pest management programs to limit agricultural pest damage requires an
23 understanding of the interactions between the environmental variability and population demographic
24 processes. However, identifying key environmental drivers of spatio-temporal pest population dynamics
25 remains challenging as numerous candidate factors can operate at a range of scales, from the field (e.g.
26 agricultural practices) to the regional scale (e.g. weather variability). In such a context, data-driven
27 approaches applied to pre-existing data may allow identifying patterns, correlations, and trends that may not
28 be apparent through more restricted hypothesis-driven studies. The resulting insights can lead to the
29 generation of novel hypotheses and inform future experimental work focusing on a limited and relevant set
30 of environmental predictors. In this study, we developed an ecoinformatics approach to unravel the multi-
31 scale environmental conditions that lead to the early re-infestation of mango orchards by a major pest in
32 Senegal, the oriental fruit fly *Bactrocera dorsalis* (BD). We gathered abundance data from a three-year
33 monitoring conducted in 69 mango orchards as well as environmental data (i.e. orchard management,
34 landscape structure and weather variability) across a range of spatial scales. We then developed a flexible
35 analysis pipeline centred on a recent machine learning algorithm, which allows the combination of gradient
36 boosting and grouped random effects models or Gaussian processes, to hierarchize the effects of multi-scale
37 environmental variables on the onset of annual BD population growth in orchards. We found that physical
38 factors (humidity, temperature), and to some extent landscape variables, were the main drivers of the spatio-
39 temporal variability of the onset of population growth in orchards. These results suggest that favourable
40 microclimate conditions could provide refuges for small BD populations that could survive, with little or no
41 reproduction, during the mango off-season and, then, recolonize neighbouring orchards at the beginning of
42 the next mango season. Confirmation of such a hypothesis could help to prioritize surveillance and preventive
43 control actions in refuge areas.

44

45 **Keywords:** *Bactrocera dorsalis*, mango crop, weather, landscape, agricultural practices, GPBoost, population
46 dynamics, abundance time series, ecoinformatics, machine learning

47 INTRODUCTION

48 Limiting pest damage is a major challenge for agriculture that has been mainly addressed through chemical
49 and curative control methods, leading to socio-economic, environmental and human health issues (Brévault
50 & Clouvel 2019; Chaplin-Kramer et al., 2011; Deguine et al., 2023; Mutamiswa et al., 2021). The need to
51 develop sustainable forms of agriculture has led to the emergence of the concept of Integrated Pest
52 Management (IPM), which aims to integrate a range of alternative pest control techniques (e.g. biological
53 control, landscape manipulation, changes in cultural practices, use of resistant varieties). However, and
54 despite decades of research in agroecology, IPM implementation often still lacks careful consideration of the
55 spatio-temporal heterogeneity of ecological processes occurring in agroecosystems (Deguine et al., 2021).
56 Indeed, demographic parameters of pest populations, although dependent on their intrinsic characteristics
57 (e.g. dispersal and reproductive capacities), are also strongly dependent on numerous environmental factors
58 that determine the spatio-temporal availability, accessibility and quality of resources, such as agricultural
59 practices, host plant diversity and phenology, natural enemies, landscape structure and weather (Kennedy &
60 Storer 2000; Veres et al., 2013). Understanding the key environmental drivers of spatio-temporal pest
61 population dynamics remains then challenging, especially in agroecosystems that are often highly labile
62 through space and time, notably due to the diversity and phenology of crops and wild hosts as well as farming
63 practices, and where different environmental variables influence demographic processes across a range of
64 spatial scales, from the field to regional scales or beyond (Brévault & Clouvel 2019; Kennedy & Storer 2000).
65 Therefore, extensive sampling efforts are required to achieve both population monitoring and environmental
66 data collection, at the relevant spatio-temporal scales and with the appropriate precision.

67 In this context, a valuable first step in investigating the ecological processes underlying pest
68 population dynamics is to create a composite set of pre-existing data, which may have been collected through
69 various research or management programs, in order to perform correlative statistical analyses. For example,
70 stakeholders often record longitudinal data on pest abundance, crop yields and farming practices, in order
71 to inform real-time pest management decisions (e.g. Rosenheim & Meisner 2013). Open access databases or
72 repositories providing raw or pre-processed data on the variability of environmental variables derived from
73 remote sensing technologies or mathematical modelling are also increasingly available (e.g. landscape
74 typologies, weather variables). Such a research framework, termed “ecoinformatics” since the era of big data
75 (Rosenheim & Gratton 2017), can capture multi-year data over large spatial extents and under environmental
76 conditions directly relevant to agriculture and management operations. For example, ecoinformatics
77 research has provided important insights on the dependencies between spatio-temporal population
78 dynamics and environmental heterogeneity for several agricultural insect pests such as aphids (Stack
79 Whitney et al., 2016), locusts (Veran et al., 2015) or plant bugs (Rosenheim & Meisner 2013). These studies
80 also provide an opportunity to inform future hypothesis-driven experimental research by (i) narrowing down
81 a large number of candidate environmental variables to a limited set of variables that are relevant to pest

82 population dynamics and amenable to experimentation and (ii) formulating more focused hypotheses on
83 causal relationships between environment and pest dynamics that can be further tested (Hochachka et al.,
84 2007; Kelling et al., 2009; Rosenheim et al., 2011).

85 The main objective of the present study was to unravel the environmental conditions that may favour
86 rapid seasonal re-infestation of mango orchards by the oriental fruit fly, *Bactrocera dorsalis* (Hendel, 1912)
87 (Diptera: Tephritidae), in Senegal. This invasive species, native from tropical Asia, has emerged as a major
88 pest of mangoes and other tropical fruit crops in Africa in the early 2000 (Ekesi et al., 2006). Direct crop losses
89 are caused by larval feeding in the fruit, but significant indirect losses occur when market access
90 opportunities are lost due to quarantine regulations (Ekesi et al., 2011; Mutamiswa et al., 2021; Vayssières
91 et al., 2008). *B. dorsalis* (BD) has a holometabolous development that goes from egg (1-2 days), larva (~7-10
92 days) in fruits, to pupa (~10–14 days) that form in the soil, before reaching adulthood and reproductive
93 maturity (~7 days) (Mutamiswa et al., 2021). Females have a high reproductive capacity with an average
94 lifetime fecundity of around 1200–1500 eggs in the field (Liu et al., 2011). Like most tephritid fruit flies, adults
95 rely on food sources such as nectar, honeydew, pollen and rotting fruits. The species has a wide host range
96 including cultivated and wild host plants (Allwood et al., 1999; Clarke et al., 2005; Ekesi & Billah 2006; Ndiaye
97 2009) but mango is the preferred cultivated host fruit (Drew et al., 2005; Ekesi et al., 2006; Motswagole et
98 al., 2019; Vayssières et al., 2009).

99 In the Niayes area, one of the main mango production basins in Senegal, the annual variation in BD
100 abundance is extremely marked, with a striking demographic bottleneck at the end of the mango season
101 raising questions about how orchards get re-infested at the beginning of the next production season. A key
102 factor could be the survival of small demes during the dry season that would constitute discreet sources to
103 initiate local population growth and rapid re-infestation of orchards at the beginning of the production
104 season. Overwintering of groups of adults in patches providing shelter and food has long been reported for
105 different species of tropical fruit flies (Bateman 1972). For BD in Senegal, many abiotic and biotic factors have
106 been identified as potentially critical for the survival of the species during the mango off-season in Senegal,
107 including temperature, precipitations, relative humidity, irrigation as well as the abundance, diversity and
108 phenology of alternative host plants within and around orchards (Boinahadji et al., 2019; Diallo et al., 2021;
109 Diatta et al., 2013; Dieng et al., 2019; Konta et al., 2015; Ndiaye et al., 2008; Ndiaye et al., 2012; Vayssières
110 et al., 2015). Population survival under unfavourable conditions has mostly been assumed to rely on
111 continuous reproduction, which explains why alternative host fruits have been the focus of many studies.
112 However, recently, Clarke et al. (2022) have suggested that BD may actually undergoes adult reproductive
113 arrest resulting in extending life span allowing population survival during unfavourable periods (e.g. scarcity
114 of host fruits).

115 Here, we first built a composite dataset from a three-year monitoring of abundance previously
116 collected in 69 mango orchards in the Niayes region (Diatta 2016) and environmental data on a large number

117 of candidate predictors at different spatial scales, including cropping systems (Diame et al., 2015; Grechi et
118 al., 2013), landscape structure (Jolivot 2021), and weather variability (Didan 2015; Karger et al., 2021). We
119 then used this dataset to assess the possible source (or sink) effects of environmental variables, by
120 investigating their relationship with the onset of annual population growth of BD within orchards. There are
121 specific analytical challenges related to the use of a large number of candidate environmental variables, such
122 as the heterogeneity in both their nature (i.e. qualitative and quantitative) and their relationship to pest
123 population dynamics (e.g. nonlinearity), as well as multicollinearity (i.e. high correlations between two or
124 more variables). Thus, we developed a flexible analysis pipeline centred on a recent machine learning
125 algorithm, GPBoost (Sigrist 2022), to integrate multi-scale candidate environmental factors and hierarchize
126 their effects. The results provided insights into the environmental conditions that may favour the rapid
127 annual re-infestation of mango orchards at the beginning of the mango production season, which can inform
128 on the favourable conditions for BD survival during the dry season. Formulated hypotheses on causal
129 relationships are discussed in relation to published experimental studies and confronted to competing
130 interpretations, in particular the potential influence of suspected confounding parameters that could not be
131 included in the study. Deciphering the relative role of environmental variables on the earliness of the re-
132 infestation process can help to prioritize future research, but also to adapt possible surveillance and
133 preventive actions for BD control.

134

135

136 **MATERIALS AND METHODS**

137

138 Figure 1 provides a schematic view of the analysis pipeline detailed in this section. All analyses were
139 performed using the R Statistical Software, version $\geq 4.1.2$ (R Core Team 2023).

140

141 **Study area**

142 The study area encompassed the “Niayes” (Figure 2), a region under Sahelian climate characterized
143 by the alternation of a short rainy season (July-September, 400-500 mm rainfall) and a long dry season
144 (October-June)(see Supplementary material, Section 4, Fig. S4.1). The Niayes is the main region of vegetable
145 and fruit production in Senegal (De Bon et al., 1997; Grechi et al., 2013). Mango is the main fruit production,
146 grew either in intensive orchards dedicated to international export or in more traditional and diversified
147 orchards for local markets (Ndiaye et al., 2012; Vayssières et al., 2011). The mango harvest season is mainly
148 from June to August and coincides with the rainy season (Grechi et al., 2013; Vayssières et al., 2011). Natural
149 vegetation is relatively scarce and forms a landscape mosaic with cultivated lands and urban areas.

150

151 Estimation of the starting date of BD population growth within orchards

152 In this study, we used BD abundance data from Diatta (2016), who monitored 69 mango orchards
153 roughly distributed among six sites in the Niayes region, between December 2011 and December 2014
154 (Figure 2). Within each orchard, an average of three traps were placed in different trees (1 to 2m height).
155 Traps were baited with methyl-eugenol, an attractive parapheromone for BD males, combined with an
156 insecticide (DDVP: dichlorvos). Male-lure has been routinely used to monitor BD populations. Manrakhan et
157 al. (2017; 2019), who monitored the abundance of both sexes over a year in South Africa, attributed the
158 earlier and higher male catches to the low attractiveness of non-specific (i.e. catching of non-target species)
159 food-baited attractants for females compared to specific methyl-eugenol baited traps for males. Another key
160 difference between methyl-eugenol and food-baited traps is the range of attraction, presumed to be about
161 500m and 30m, respectively. Male trapping systems are generally recommended for early detection and
162 estimation of BD abundance while food-based baits may be more indicative of the threat of female flies as
163 the fruit ripens (Manrakhan et al., 2017; Manrakhan et al., 2019), and are closely linked to sexual maturity
164 stage and degree of protein need (Epsky et al., 2014; Vargas et al., 2018). The traps were collected once a
165 week and the number of flies caught was counted from each trap placed in each orchard. For each orchard
166 and sampling date, the number of flies caught was averaged across all traps in order to obtain abundance
167 time series.

168 Then, for each orchard and year, we estimated the starting date (as the number of weeks from first
169 of January) of the demographic growth of local BD populations using the POPFIT mechanistic model (Soulsby
170 & Thomas 2012; see details in Supplementary material, Section 1). Originally developed for butterfly species,
171 POPFIT can be applied to others insect species with similar annual population dynamics, as observed from
172 BD abundance time series: a phase of zero or almost zero abundance followed by a phase of rapid population
173 growth to a peak and then a decline to zero abundance again (Figure 3). The initial hypotheses of the POPFIT
174 model were relaxed as we were only interested in estimating the onset of the demographic growth phase
175 (t_0) regardless of the underlying demographic processes (adult survival from one year to the next, local
176 eclosions, migration or a combination of these processes). A mechanistic-statistical framework was used to
177 perform the parameter inference of the POPFIT model (Papaïx et al., 2022) within a Bayesian framework
178 using Nimble (de Valpine et al., 2017) with the R package “nimble” v. 1.0.1 (see details in Supplementary
179 material, Section 1). The Bayesian inference provided one posterior distribution of plausible t_0 values given
180 the data for each combination of orchard and year. Markov chain Monte Carlo (MCMC) convergence was
181 checked based on both, a visual assessment of the trace plots of the chains and the computation of the
182 Gelman-Rubin statistic. To further check whether the estimated model adequately fits the data, we visually
183 compared the simulated data and the observations. Then, we completely removed orchards for which the
184 MCMC convergence was not reached or the abundance time series appeared to be unreliable for at least one
185 year. Finally, for each remaining orchard and year, we randomly resampled 500 values of the t_0 parameter

186 from the posterior distributions. These values were then associated to build 500 sample sets of t_0 , each of
187 them including a single value of t_0 for each combination of orchard and year. This procedure, which contrasts
188 with a more classical approach consisting in extracting a single point value of the posterior distributions
189 (either mean, median or mode), allows to consider the range of plausible values of t_0 given the data and,
190 then, to account for the uncertainty of the estimation in further analyses in which this parameter is the input
191 response variable (see Supplementary material, Section 5A, Fig. S5.1 for a graphic illustration of the building
192 of the 500 sample sets of t_0).

193

194 **Multi-scale environmental predictors**

195 *Within orchards.* Between 2010 and 2013, the cropping system of 86 orchards, including the 69 orchards
196 monitored for BD abundance that we analysed in the present study, was characterized using the same
197 methodology (Diame et al., 2015; Diatta 2016; Grechi et al., 2013). Mango producers were interviewed about
198 the management of their orchard, particularly on practices that might affect early BD population growth
199 within orchards: irrigation, sanitation (i.e. removal of aborted mangoes that can host BD larvae) and
200 intercropping with vegetable crops as potential alternative hosts for BD (Diouf et al., 2022; Grechi et al., 2013;
201 Vayssières et al., 2015). These factors were considered as qualitative variables: irrigation and sanitation as
202 factors with three levels (null, moderate or intensive irrigation and null, occasional or regular sanitation) and
203 inter-crops as presence/absence. In the Niayes, orchards can consist entirely of mango trees or be mixed
204 with other fruit trees, such as citrus, papaya or guava, which are potential alternative hosts for BD (Grechi et
205 al., 2013). Then, host diversity and frequency, which may also influence BD re-infestation dynamics
206 (Boinahadji et al., 2019; Diallo et al., 2021; Diatta 2016; Grechi et al., 2013; Ndiaye et al., 2012; Vayssières et
207 al., 2011), were estimated from a subset of around 100 fruit trees per orchard. Each selected tree was
208 identified at the species level and for mango trees, the cultivar was also identified.

209 Here, agricultural practices (irrigation, sanitation, intercropping with vegetables) were kept as
210 categorical variables. Due to the high number of fruit tree species and mango cultivars identified in the
211 orchards and the bias in the representation of some categories (i.e. from only one sample for the rarest
212 category to nearly 2000 for the most frequent category), we classified both the mango cultivars and the
213 alternative host tree species according to their phenology, especially the period during which fruits are
214 available and can potentially host BD larvae, based on data from literature and expert knowledge (from
215 researchers and producers). For mango trees, we individualized the three main cultivars (Kent, Keitt,
216 Boukodiekhall) and grouped the others in three phenological classes (early, medium, late). For other species,
217 we grouped them into three classes according to their potential period of fruit availability: December to April
218 (before the beginning of the mango season), April to November (during and after the mango season), and all
219 year round. Then, for each orchard, we calculated the proportion of each phenological class by dividing the

220 number of trees in a class by the total number of trees sampled in the orchard (see details on host diversity
221 and phenology in Supplementary material, Section 2, Tab. S2.1).

222

223 *Landscape.* To quantify the effect of the landscape variables surrounding the monitored orchards on the
224 onset of BD population growth, we used a pre-existing typology of 13 classes of land use (Figure 2) built using
225 2010-SPOT6 satellite images and time series of 2018-Sentinel 2 satellite images (Jolivot 2021). The effect of
226 landscape variables surrounding plots monitored to record population abundance is often investigated using
227 nested circular buffers or rings of increasing radius, but such approaches have drawbacks such as the high
228 level of correlation of landscape variables across the different radii considered and the rather unrealistic
229 assumption that landscape effects are uniform within a given buffer and null outside (Carpentier & Martin
230 2021; Chandler & Hepinstall-Cymerman 2016). In this work, we used the recent Siland method (Carpentier &
231 Martin 2021), which allows to estimate the spatial scale of influence of a landscape feature on a response
232 variable (here t_0), without any a priori of distance. The method also allows to consider local explanatory
233 variables: here we included the sampling year and site. The spatial influence function (SIF), which models the
234 decreasing influence with distance from the observation points of the landscape variables, was a Gaussian
235 function with a mean distance δ , estimated with Siland independently for each of the 13 land use classes.
236 Based on the estimated value of δ , Siland provided the cumulative influence of each land use class at each
237 observation point, i.e. the land contribution, hereafter denoted as lc .

238 We first carried out a sequential tuning step of the Siland hyperparameters: the raster resolution wd
239 and the initialisation value for the maximum likelihood optimization procedure *init* (see Supplementary
240 material, Section 3). Then, lc values were computed independently for each of the 500 sample sets of t_0 .
241 Analyses were performed using the R package “siland” v. 3.0.2 (Carpentier & Martin 2021).

242

243 *Regional weather variability.* The spatio-temporal variability of physical factors was analysed over the study
244 area and the period of sampling using two data sources. First, we used raster data of monthly minimal,
245 maximal and mean temperatures (Tmin, Tmax, Tmean), as well as precipitations, obtained from the *CHELSA*
246 model v. 2.1 (Karger et al., 2017; Karger et al., 2021) with a spatial resolution of 30 arc-seconds
247 (approximately 1 km). Second, we used rasters of bi-monthly Normalized Difference Water Index (NDWI), an
248 indicator for vegetation water content (Gao 1996; Gu et al., 2007) that we calculated using MODIS/Terra
249 Vegetation Indices 16-Day L3 Global 250m SIN Grid data (Didan 2015; Didan et al., 2015) according to the
250 formula of $NDWI_{2130}$ defined in Chen et al. (2005). NDWI data were averaged monthly and combined with
251 *CHELSA* data to obtain monthly raster time series of 1 km² spatial resolution covering the entire study area.
252 We only kept the rasters for the time period between December and May, which covers the low demographic
253 phase preceding population growth for each sampling year (i.e. Dec 2011–May 2012, Dec 2012–May 2013
254 and Dec 2013–May 2014, thereafter named 2012, 2013 and 2014 for the sake of simplicity). The final dataset
255 was composed of 30 variables (6 months x 5 variables: Tmin, Tmax, Tmean, precipitations and NDWI),

256 computed for each of the 2863 cells (1 km²) of the spatial raster and for each year; i.e. a matrix of size 30 x
257 8589. Data were normalized and reduced in a smaller dimensional space using a principal component analysis
258 (PCA). For each monitored orchard and each of the main principal components (PC), selected using the
259 Broken Stick model (MacArthur 1957), we extracted the PC scores of the grid cell corresponding to the spatial
260 location of the orchard in the study area (three values, one per year). The analyses were performed using the
261 R packages “ade4” v. 1.7-19 (Dray & Dufour 2007) and “PCDimension” v. 1.1.13 (Wang et al., 2018).

262

263 **Effect of multi-scale environmental factors on the onset of local BD population growth**

264 To hierarchize the effects of the multi-scale environmental predictors on the onset of demographic
265 growth of BD populations in orchards (t_0), we used the recent tree-boosting method GPBoost (Sigrist 2022).
266 Boosting methods can handle high-dimensional data, i.e. number of variables larger than the number of
267 observations (Bühlmann & Hothorn 2007; Rosset et al., 2004). Tree-boosting also generally provides the
268 highest prediction accuracy among machine learning methods (Grinsztajn et al., 2022; Johnson & Zhang 2013;
269 Nielsen 2016). GPBoost has the further advantage of allowing a direct combination of gradient tree boosting
270 with grouped random effects models or/and Gaussian processes to account for dependencies in the
271 observations. The joint estimation of the Gaussian process and the mean function has notably been shown
272 to be more efficient than the two-step approach required for the combination of random forest and Gaussian
273 process (Sigrist 2022). Based on simulated and real data, Sigrist (2022) also showed that for mixed effect
274 models, the GPBoost algorithm resulted in the highest prediction accuracy, compared to a range of statistical
275 and machine learning methods such as linear models, gradient boosting with a square loss including the
276 grouping variable as a categorical variable or random forest.

277 All environmental candidate factors were considered as fixed effects: i) the 12 orchard management
278 variables (i.e. irrigation, sanitation, vegetable crops, and phenological groups of mango trees and alternative
279 hosts), ii) the contributions (lc) of the 13 land use classes estimated with Siland and, iii) the scores for each
280 orchard on the retained PCs of the PCA conducted on the physical variables (i.e. minimum, maximum and
281 mean temperatures, precipitations and NDWI) (see Supplementary material, Section 5A, Tab. S5.1 for a more
282 detailed description of these variables). Analyses were conducted using the R package “gpboost” v. 1.2.3
283 (Sigrist 2023). We first tested seven GPBoost models considering various combinations of grouped random
284 effects and Gaussian process (see details in Supplementary material, Section 5B). Based on model Mean
285 Square Error (MSE) values, we retained the GPBoost regression model including the sampling site (S1 to S6)
286 and year (2012, 2013 and 2014) as grouped random effects (see Model 1 in Supplementary material, Section
287 5B). Considering this model, we performed 500 independent analyses on the 500 different sample sets of t_0
288 estimates as follows. For each sample set, GPBoost model hyperparameters (the learning rate, the minimum
289 data number in tree leaves, the maximal depth of trees and the number of trees) were tuned using the grid
290 search procedure implemented in the package “gpboost” and based on a 4-fold cross-validation (see details

291 in Supplementary material, Section 5B). For the number of trees, it was automatically optimized by setting
292 the maximum number of iterations to 2000 and the *early_stopping_rounds* parameter to 5, i.e. the process
293 stops if the model's performance on the validation set does not improve for five consecutive iterations. The
294 model was then trained with the “*gpboost*” function using the best combination of hyperparameter values
295 identified for the sample set in the tuning step, and the predictors were hierarchized according to their
296 importance in the model expressed by the SHapley Additive exPlanation (SHAP) values (Lundberg & Lee 2017;
297 Lundberg et al., 2018), computed using the R package “SHAPforxgboost” v. 0.1.1 (Liu & Just 2021). SHAP
298 values provide the contribution of each predictor on the predicted values of individual observations. The
299 overall contribution of a given predictor to the model output is obtained by averaging the absolute SHAP
300 values of the observations (hereafter called S_{mean}).

301 The predictors were then ranked in decreasing order by computing the median of their S_{mean} values
302 over all 500 analyses. Based on this ranking, the relationship of each of the most important predictors with
303 the estimated t_0 was investigated using a dependence plot built by fitting individual SHAP values from the
304 500 analyses as a gam-smoothed function of the predictor values, using the R package “mgcv” v.1.9-1 (Wood
305 2017).

306 Finally, as a validation step of the variable selection procedure, we assessed the predictive
307 performance of the GPBoost model considering either all predictors or the top ranked predictors. In both
308 cases, we performed 500 independent analyses on the 500 different sample sets as follows. First, partitioning
309 of the sample set was done in a way to build random training and test datasets (80% and 20% of the data,
310 respectively) while ensuring that all years and sites (i.e. groups of random effects) were represented at least
311 once in the training dataset. Second, the GPBoost model was tuned and trained on the training dataset as
312 previously detailed (see Supplementary material, Section 5B), and the resulting model was used to predict t_0
313 from the corresponding test dataset. Finally, model accuracy was assessed by computing the Pearson
314 correlation coefficient between predicted and observed values of t_0 as well as the Root Mean Square Error
315 (RMSE) of the model for each sample set.

316 An overview of the main analysis steps with GPBoost is presented in Supplementary material, Section
317 5A, Fig S5.1.

318

319

320 RESULTS

321 As described in Diatta (2016), the BD abundance time series showed an annual demographic kinetics
322 consistent with the use of the POPFIT model (Figure 3). As for the Bayesian estimation of the start date of
323 the population growth (i.e. t_0 parameter), all but four orchards achieved MCMC convergence and displayed
324 a good fit to the data for the three years (see details in Supplementary material, Section 1). These four

325 orchards were all located within site S2 (Figure 2) and discarded for further analyses. The distributions of the
326 500 t_0 samples drawn from the Bayesian posterior distributions for each of the 65 remaining orchards and
327 for each of the 3 years (i.e. 195 combinations) showed an overall high precision of the estimation with the
328 POPFIT framework (Supplementary material, Section 1, Fig. S1.1). The difference between the maximum and
329 minimum values of the 500 samples of the t_0 parameter for a combination of orchard and year was 0.7 weeks
330 on average (i.e. over all combinations of orchard and year).

331 Results over the 500 independent analyses of the GPBoost model applied to the 500 sample sets
332 showed that the median and range values for the error term and grouped random effects (i.e. *year* and *site*),
333 were 0.4 [0; 1.72], 1.86 [0.72; 3.03] and 0.14 [0; 1.64] weeks, respectively. A significant proportion of the
334 variance in t_0 is then expected to be explained by fixed effects. Indeed, within-year variation of t_0 between
335 orchards was substantial, with a difference between the earliest and the latest orchard (i.e. the difference in
336 the median of the within-orchard t_0 values over the 500 sample sets) of 12, 17 and 15 weeks in 2012, 2013
337 and 2014, respectively. This means that the earliest onset of BD population growth was in March (2013) or
338 April (2012 and 2014) and the latest in June (2012) or July (2013, 2014). For a same orchard, the variation in
339 the median of the t_0 values (over the 500 sample sets) between years was, on average over all orchards and
340 years, 3.4 weeks. The results of the SHAP-based ranking over the 500 sample sets for the 28 environmental
341 predictors specified as fixed effects in the GPBoost model are presented Figure 4. From this ranking, two
342 groups of predictors stand out as the most meaningful to explain the variability in the annual onset of BD
343 population growth (t_0) within orchards. The first group included the three first principal components
344 (predictors PC3, PC2 and PC1) retained by the broken stick method, which explained 77.8% of the total
345 variance in the PCA performed on the physical variables (i.e. temperatures, precipitations and NDWI; Figure
346 5A), as well as the land use class LU13 (urban area). The second group of variables included two additional
347 land use classes, LU7 (shrub savannah) and LU11 (sparsely vegetated ground) as well as an agronomic feature
348 of the studied orchards, i.e. the proportion of potential alternative hosts producing fruits between April and
349 November (AH3).

350 The top ranked predictor was the third principal component of the PCA (PC3), which was negatively
351 correlated with the vegetation water content index (NDWI) from December to May, and mainly reflected fine
352 spatial variation of NDWI values over these months (Figures 5A, 5B). The SHAP-dependence plot (Figure 6)
353 showed a positive relationship between PC3 values and the individual SHAP values (i.e. negative SHAP values
354 for the lowest PC3 values and positive SHAP values for highest PC3 values), meaning that earlier start dates
355 of BD population growth (t_0) in orchards were associated with higher values of NDWI, i.e. humidity. The
356 second-best predictor was PC2 (Figure 4). This component of the PCA was a temporal dimension, which
357 contrasted humidity conditions: positive values were correlated with precipitations occurring between
358 February and April and with higher NDWI values between December and May, while negative values were
359 correlated with precipitations in December, January and May (Figure 5A). The former conditions were mainly
360 observed in 2012 and, to a lesser extent, in 2013 while the later mostly corresponded to the year 2014 (Figure

361 5B). Although the SHAP dependence plot for the PC2 predictor showed a sawtooth-kind of relationship
362 (Figure 6), there was a clear trend indicating that negative individual SHAP values roughly corresponded to
363 positive PC2 values. This result suggests that **BD population growth (t_0) in orchards is expected to start** earlier
364 when humidity conditions (precipitations and NDWI) are higher between February and April. **The third best**
365 **predictor** was the first component of the PCA (PC1), which showed a well-marked spatial gradient in monthly
366 temperature ranges, from positive values in the coastal area, associated with the highest minimum
367 temperatures and the lowest maximum temperatures, to negative values in the inland, characterized by the
368 highest maximum temperatures and lowest minimum temperatures (Figures 5A, 5B). Smoothed SHAP-values
369 associated with PC1 exhibited a U-shaped curve (Figure 6), suggesting that the earliest **starts of BD population**
370 **growth (t_0) in orchards** are associated with intermediate conditions in terms of minimum and maximum
371 monthly temperatures, as observed in the central part of the study area. Three other top predictors identified
372 from the ranking of the results over the 500 different GPBoost analyses **applied on the 500 sample sets**
373 corresponded to landscape classes (Figure 4), expressed in terms of cumulative influence (I_c) on estimates of
374 t_0 as computed with the Siland method (see Supplementary material, Section 3, Tab. S3.1 for a detailed
375 description of Siland results). The smoothed relationships between these landscape predictors and the
376 individual SHAP values (Figure 6) roughly approximated either: an L-shaped or inverted L-shaped curve for
377 urban area (LU13) and sparsely vegetated ground (LU11) respectively, and a S-shaped curve for shrub
378 savannah (LU7). These relationships suggest that the presence of urban areas (LU13) in the orchard's
379 surrounding is associated with early population growth (i.e. smallest t_0 values). On the contrary, the presence
380 of sparsely vegetated ground (LU11) and shrub savannah (LU7) tend to delay the onset of the demographic
381 growth of BD populations within orchards (i.e. highest t_0 values). Finally, the smoothed SHAP curve for the
382 class of potential alternative hosts AH3 **(i.e. grouping species having fruits mostly during and/or after the**
383 **mango season in the Niayes, from April to November: Annona species, cashews, guava, pomegranate and**
384 **kola nuts, see Supplementary material, Section 2, Tab S2.1)** also approximated an inverted L-shaped
385 relationship suggesting that the higher the proportion of these tree species, the later the onset of BD
386 population growth within orchards.

387 Lastly, as a validation step of our variable selection procedure, we assessed the predictive
388 performance of the GPBoost model considering either all predictors, the seven top ranked predictors (i.e.
389 PC3, PC2, PC1, LU13, LU11, LU7, AH3) or only the four top ranked predictors (i.e. PC3, PC2, PC1 and LU13).
390 The RMSE and Pearson correlation coefficient, averaged over the 500 analyses, were 2.24 and 0.77,
391 respectively, for the model including all predictors, 2.23 and 0.78 for the model including seven predictors
392 and 2.23 and 0.77 for the model including the four top predictors (see details in Supplementary material,
393 Section 5C, Fig. S5.3).

394
395

396 DISCUSSION

397 In this work, we present a flexible analysis pipeline to hierarchize the effects of multi-scale candidate
398 environmental factors on estimated parameters of pest population dynamics (Figure 1). At the heart of this
399 pipeline is a recent machine learning method, GPBoost, which allows gradient boosting to be combined with
400 mixed effects models or latent Gaussian models (Sigrist 2022). The method inherently benefits from the
401 advantages of gradient-boosted trees (e.g. handling of nonlinearities, discontinuities, higher order
402 interactions, outliers, multicollinearity between predictors and missing data (Elith et al., 2008)), while
403 allowing to relax the zero prior mean or linearity assumption of Gaussian process and mixed effects models
404 (Sigrist 2022). The possibility to consider grouped random effects, as done in the present study, also provides
405 a unique way to account for the non-independence of the response variable across observations, which is
406 overlooked in most machine learning algorithms. This pipeline allowed us to integrate pre-existing data from
407 multiple sources to hierarchize the effects of 28 environmental predictors, assessed from the local to the
408 regional scale, on the annual onset of local population growth (t_0) of *Bactrocera dorsalis*, a major invasive
409 pest of the mango crop in Senegal.

410 Given that the two best environmental predictors were the third and second principal components
411 of the PCA carried out on physical variables, our results clearly suggest that humidity conditions are the
412 primary driver of the spatio-temporal variation in the earliness of local population growth of BD in mango
413 orchards of the Niayes region (i.e. up to 17 weeks of delay between the earliest and latest onset of the local
414 population growth within a year). This result is in line with previous studies reporting humidity as a key
415 component of BD population dynamics (e.g. Chuang et al., 2014; Ibrahim et al., 2022; Vayssières et al., 2009).
416 The relationship between the estimated **start of local population growth** (t_0) and **the variation in monthly**
417 **precipitations (predictor PC2)**, indicated that even a very small episodic rainfall event occurring before the
418 mango season between February and April (Figure 5A) (which are called “heug” or “mango rain” in Senegal
419 (Wade et al., 2015)) could be involved in creating favourable conditions leading to early development of BD
420 populations in orchards. Furthermore, the fine variation in **space and time of the level of humidity, expressed**
421 **by the Normalized Difference Water Index (NDWI), was the best predictor (PC3) of the start date of**
422 **population growth within orchard. Early onsets of population growth were associated with high values of**
423 **NDWI, which depends, at least partly, on precipitations and soil moisture.** These results are consistent with
424 several experimental studies indicating that humidity is a critical factor for BD survival, especially at the pupal
425 stages. Indeed, the survival of pupae (and so the emergence rate) is significantly affected by soil moisture,
426 which is strongly related to precipitations, with optimal trait values at 10-60% moisture levels (Hou et al.,
427 2006). Desiccation is also an important cause of mortality of third-instar larvae under different climatic
428 conditions (Jackson et al., 1998; Serit & Tan 1990). Furthermore, from observational data in Penang,
429 Malaysia, Serit & Tan (1990) found that the main factors of mortality of BD immature stages was desiccation

430 or drowning of larvae and pupae in soil (77.8% of mortality for soil-associated immatures). In this way, BD
431 larvae's preference for pupating in shaded areas has already been mentioned (Susanto et al., 2022).

432 Importantly, the vegetation water content (NDWI) also reflects the vegetation fraction cover (i.e.
433 importance of the canopy). Thus, higher NDWI values may also reflect favourable microclimate conditions
434 for adults of BD, with higher moisture levels and higher shading effects that will contribute to moderate
435 temperature variations. Besides, the first component of the physical PCA, which showed a gradient in
436 minimum and maximum monthly temperatures, was also ranked in the top environmental predictors with
437 intermediate conditions of temperature associated with the earliest BD population growth. This result would
438 be consistent with previous experimental studies describing performance curves for temperature-dependent
439 development, survival and fecundity traits in *B. dorsalis*. For example, temperatures for optimal immature
440 development ranged around 25-30°C, with development time (or mortality) increasing at lower (or higher)
441 temperatures, preventing from any adult emergence above 35°C (and below 9-10°C) (Dongmo et al., 2021;
442 Rwomushana et al., 2008; Vargas et al., 1996). In addition, adult longevity decreases with increasing
443 temperature, and females can only lay eggs between 15 and 35°C, with the optimal conditions for a higher
444 number of eggs being between 20 and 25°C (Choi et al., 2020; Dongmo et al., 2021; Vargas et al., 1997; Yang
445 et al., 1994). In our study area, the most favourable temperature range for early population development in
446 orchards lies between oceanic conditions in the coastal part and inland conditions where the maximum daily
447 temperature easily exceeds 35°C during the dry season. As temperatures above 35°C challenge all
448 components of BD life history, spatial and inter-annual weather variability in the Niayes region is likely to
449 interact with local factors providing higher levels of humidity and shading (e.g. water bodies and
450 groundwater, vegetation and soil moisture, canopy structure) to create favourable habitats allowing BD to
451 mitigate hydric and thermal stress during the dry season (Inskeep et al., 2021; Mutamiswa et al., 2021).

452 In addition to physical factors, the boosting approach also identified three landscape variables that
453 influenced the timing of the annual re-infestation of mango orchards. First, urbanized areas (LU13) would act
454 as a catalyst for early re-infestation. This phenomenon could be attributed to the high frequency of peri-
455 urban farming or even micro-gardens within towns. Intensive irrigation practices and the presence of
456 alternative host plants, like citrus, during the dry season in these areas (Vayssières et al., 2011) might offer
457 favourable conditions for BD survival and reproduction. The role of urban area in sustaining populations has
458 been pointed out for other fly pest species, such as *Drosophila suzukii*, under unfavourable northern climates
459 (e.g. Dalton et al., 2011; Rossi-Stacconi et al., 2016) and, very recently, for *Ceratitis capitata* in Australia,
460 where unmanaged urban populations have been estimated to contribute to pest pressure in surrounding
461 orchards up to 2 km (Broadley et al., 2024). Another non-exclusive plausible explanation relies on the
462 potential contribution to local population dynamics of flies originating from imported mangoes in the region
463 (Hong et al., 2015; Louzeiro et al., 2021). Before the start of the production season in the Niayes, mangoes
464 are massively imported from southward production basins (e.g. Guinea, Southern Mali and Casamance) to
465 supply the local markets including those in the study area. The arrival of potentially infested mangoes could

466 contribute to the early establishment of a pool of individuals, which may then lead to the rapid re-infestation
467 of nearby orchards. Second, the presence of sparsely vegetated ground (LU11) and shrub savannah (LU7)
468 would conversely delay the onset of local population growth. These landscape classes may be unsuitable
469 habitats for BD due to the absence of host plants and the very low relative humidity, soil moisture and
470 shading. Re-infestation of orchards surrounded by these types of habitats might strongly rely on BD dispersal
471 from favourable refuges, a process that may be limited under dry conditions, leading to delays in re-
472 infestation. Habitats such as shrub savannah may also shelter natural enemies that could impact BD
473 abundance and dispersal (Vayssières et al., 2016).

474 Although considered to be significant factors impacting BD population dynamics, we did not identify
475 any clear effect suggesting that orchard management could determine the timing of the clear change in BD
476 abundance, either in terms of agricultural practices (irrigation, sanitation and presence of vegetable crops)
477 or host diversity (mango varieties and alternative hosts) and phenology. The only potential effect found was
478 that an increasing proportion of the alternative host class AH3, which produce fruits mainly during the mango
479 season (April to November), would delay the onset of BD population growth within orchards, which may
480 reflect the strong preference of BD for mango. In contrast to previous studies that have investigated BD
481 population dynamics strictly in terms of abundance variation, we specifically focused on the onset of local
482 population growth. Thus, our results suggest that while orchard management may explain differences in
483 abundance, it plays a far less important role in initiating the re-infestation process compared to physical and
484 landscape variables. However, one methodological point worth noticing is that the orchard management
485 data we used in our analysis was only available for monitored orchards (no information about practices in
486 the surroundings) and some were coded as categorical variables with a few levels, which may not allow us to
487 properly capture the underlying relationships between categories. Such categorical variables may also be
488 much less informative than continuous predictors to find optimal split points for decision trees in the gradient
489 boosting procedure.

490 Mango is the preferred cultivated host fruit of BD (Drew et al., 2005; Ekesi et al., 2006; Motswagole
491 et al., 2019; Vayssières et al., 2009), but the species is known to be highly polyphagous (Allwood et al., 1999;
492 Clarke et al., 2005; Ekesi & Billah 2006; Ndiaye 2009), which has led to the assumption that its maintenance
493 during the dry season relies on the presence of alternative hosts to ensure continuous reproduction and
494 larval development (Boinahadji et al., 2019; Diallo et al., 2021; Diatta 2016; Faye et al., 2021; Ndiaye et al.,
495 2012; Vayssières et al., 2015). However, although 34 species of host fruit trees have been reported in the
496 arid to semi-arid environment of the Niayes region (Ndiaye et al., 2012), their availability during the dry
497 season remains relatively erratic, with the exception of cultivated *Citrus spp.*. Thus, one possible explanation
498 for the lack of evidence for a role of alternative hosts in the earliness of orchard re-infestation is that the
499 underlying process involved in BD maintenance during the mango off-season in the Niayes region may not
500 be a continuous reproduction. This explanation is supported by the good performance of the GPBoost model
501 in predicting the onset of the BD population growth in orchards based only on a few environmental factors

502 representing physical and landscape variables. Active dispersal and dormancy are alternative ways of coping
503 with stress during the unfavourable season. Experimental studies have shown that the dispersal of *B. dorsalis*
504 adults is quite spatially restricted, generally upwind and occurs mostly when resources are scarce and
505 temperatures exceed 20-24°C (Chailleux et al., 2021; Froerer et al., 2010; Makumbe et al., 2020). Dormancy
506 is the interruption or reduction of metabolic and developmental activity in an immediate (quiescence) or pre-
507 programmed (diapause) response to unfavourable conditions. While pupal dormancy is a common aridity
508 survival strategy in Dipteran species (Thorat & Nath 2018), it has not been demonstrated in a *B. dorsalis*
509 desiccation experiment (Hou et al., 2006). Clarke et al. (2022) argue that phenological data on tropical
510 *Bactrocera spp.* strongly suggest an adult reproductive arrest that would allow life span to be extended during
511 the unfavourable dry season when fruits are scarce. This hypothesis of an adaptation to survive desiccation
512 during the dry season fits well with our main findings that habitat characteristics underlying early population
513 growth rates are those that provide milder temperatures and higher humidity and shading.

514 It should be noted that the data used in this study have some limitations. First, the data describing
515 the cropping system (i.e. host plant diversity and agricultural practices) may not be precise enough to detect
516 significant effects in statistical analyses. Second, pre-existing demographic data are limited to the abundance
517 of BD in orchards clustered in six sites, which does not allow to investigate whether the variability in the
518 timing of re-infestation also depends on BD dispersal processes in interaction with the environmental matrix.
519 Further research is therefore needed, based on better spatial coverage and finer data collection, to assess
520 environmental heterogeneity (from the orchard to the regional scale) and its impact on the spatio-temporal
521 dynamics of BD. Moreover, the acquisition of longitudinal demographic data would be a crucial advance,
522 allowing the estimation of spatio-temporal interactions between variations in effective densities, population
523 sizes and dispersal patterns.

524 Despite these limitations, our results indirectly provide valuable insights into the spatial and temporal
525 conditions that may lead to the emergence of local habitats favourable to BD survival during the dry season
526 in the Niayes. Altogether, our results support the hypothesis of localised refuges, with more favourable
527 conditions of temperature (moderate), humidity (high) and shade (high), where small BD populations could
528 survive and re-infest orchards at the beginning of the mango season. If confirmed in future experimental and
529 observational studies, such an information could ultimately be a key step for the design of surveillance
530 programs and preventive control measures. Considering the large delay between the earliest and the latest
531 onset of population growth found in this study (between 12 and 17 weeks depending on the year), locating
532 areas with such favourable environmental conditions could allow preventive control measures to be taken
533 during the dry season to limit the sources of orchard re-infestation.

534 **Acknowledgements**

535 We would like to deeply thank the Senegalese producers who welcomed the monitoring of BD dynamics in
536 their orchards and participated in the construction of the data set analysed in this work. We are thankful to
537 the CBGP computing and data management platform and the genotoul bioinformatics platform Toulouse
538 Occitanie (Bioinfo Genotoul, <https://doi.org/10.15454/1.5572369328961167E12>) for providing computing
539 and storage resources. We are grateful to K. Tougeron, J. Sun, as well as the recommender E. Vercken, for
540 their constructive comments on an earlier version of this preprint.

541

542 **Funding**

543 This work was supported by the DISLAND project, publicly funded by the ANR (Projet-ANR-20-CE32-0012).
544 CC's doctoral fellowship was complemented by the French Agricultural Research Centre for International
545 Development (CIRAD).

546

547 **Conflict of interest disclosure**

548 The authors of this preprint declare that they have no conflict of interest relating to the content of this article.
549 KB and JP are recommenders for PCI Ecology; SP contributes to the development of PCI websites.

550

551 **Supplementary material**

552 Supplementary material is available from BioRxiv, DOI: 10.1101/2023.11.10.566583

553

554

555 **REFERENCES**

- 556 Allwood AJ, Chinajariyawong A, Drew RAI, Hamacek EL, Hancock DL, Hengsawad C, Jipanin JC, Jirasurat M,
557 Kong Krong C, Kritsaneepaiboon S, Leong CTS, Vijaysegaran S (1999) Host plant records for fruit flies
558 (Diptera: Tephritidae) in Southeast Asia. *Raffles Bulletin of Zoology*, **47**, 1-92.
- 559 Bateman MA (1972) The Ecology of Fruit Flies. *Annual Review of Entomology*, **17**.
560 <https://doi.org/10.1146/annurev.en.17.010172.002425>
- 561 Boinahadji AK, Coly EV, Dieng EO, Diome T, Sembene PM (2019) Interactions between the oriental fruit fly
562 *Bactrocera dorsalis* (Diptera, Tephritidae) and its host plants range in the Niayes area in Senegal. *Journal*
563 *of Entomology and Zoology Studies*, **7**, 855-864.
- 564 Brévault T, Clouvel P (2019) Pest management: Reconciling farming practices and natural regulations. *Crop*
565 *Protection*, **115**, 1–6. <https://doi.org/10.1016/j.cropro.2018.09.003>

- 566 Broadley A, Van Klinken RD, Paini DR, Hill M, Howse E (2024) A spatio-temporal modelling approach to
567 understand the effect of urban fruit fly outbreaks on peri-urban orchards. *Ecological Informatics*, **80**,
568 [102536. https://doi.org/10.1016/j.ecoinf.2024.102536](https://doi.org/10.1016/j.ecoinf.2024.102536)
- 569 Bühlmann P, Hothorn T (2007) Boosting Algorithms: Regularization, Prediction and Model Fitting. *Statistical*
570 *Science*, **22**, 477-505. <https://doi.org/10.1214/07-STS242>
- 571 Carpentier F, Martin O (2021) Siland a R package for estimating the spatial influence of landscape. *Scientific*
572 *Reports*, **11**, 7488. <https://doi.org/10.1038/s41598-021-86900-0>
- 573 Chailleux A, Thiao DS, Diop S, Bouvery F, Ahmad S, Caceres-Barrios C, Faye E, Brévault T, Diatta P (2021)
574 Understanding *Bactrocera dorsalis* trapping to calibrate area-wide management. *Journal of Applied*
575 *Entomology*, **145**, 831–840. <https://doi.org/10.1111/jen.12897>
- 576 Chandler R, Hepinstall-Cymerman J (2016) Estimating the spatial scales of landscape effects on abundance.
577 *Landscape Ecology*, **31**, 1383–1394. <https://doi.org/10.1007/s10980-016-0380-z>
- 578 Chaplin-Kramer R, O'Rourke ME, Blitzer EJ, Kremen C (2011) A meta-analysis of crop pest and natural enemy
579 response to landscape complexity: Pest and natural enemy response to landscape complexity. *Ecology*
580 *Letters*, **14**, 922–932. <https://doi.org/10.1111/j.1461-0248.2011.01642.x>
- 581 Chen D, Huang J, Jackson TJ (2005) Vegetation water content estimation for corn and soybeans using spectral
582 indices derived from MODIS near- and short-wave infrared bands. *Remote Sensing of Environment*, **98**,
583 225–236. <https://doi.org/10.1016/j.rse.2005.07.008>
- 584 Choi KS, Samayoa AC, Hwang S-Y, Huang Y-B, Ahn JJ (2020) Thermal effect on the fecundity and longevity of
585 *Bactrocera dorsalis* adults and their improved oviposition model. *PLoS ONE*, **15**, e0235910.
586 <https://doi.org/10.1371/journal.pone.0235910>
- 587 Chuang C-L, Yang E-C, Tseng C-L, Chen C-P, Lien G-S, Jiang J-A (2014) Toward anticipating pest responses to
588 fruit farms: Revealing factors influencing the population dynamics of the Oriental Fruit Fly via automatic
589 field monitoring. *Computers and Electronics in Agriculture*, **109**, 148–161.
590 <https://doi.org/10.1016/j.compag.2014.09.018>
- 591 Clarke AR, Armstrong KF, Carmichael AE, Milne JR, Raghu S, Roderick GK, Yeates DK (2005) Invasive
592 Phytophagous Pests Arising Through A Recent Tropical Evolutionary Radiation: The *Bactrocera dorsalis*
593 Complex of Fruit Flies. *Annual Review of Entomology*, **50**, 293–319.
594 <https://doi.org/10.1146/annurev.ento.50.071803.130428>
- 595 Clarke AR, Leach P, Measham PF (2022) The Fallacy of Year-Round Breeding in Polyphagous Tropical Fruit Flies
596 (Diptera: Tephritidae): Evidence for a Seasonal Reproductive Arrestment in *Bactrocera* Species. *Insects*,
597 **13**, 882. <https://doi.org/10.3390/insects13100882>
- 598 Dalton D & Walton V, Shearer P, Walsh D, Caprile J, Isaacs R (2011) Laboratory survival of *Drosophila suzukii*
599 under simulated winter conditions of the Pacific Northwest and seasonal field trapping in five primary
600 regions of small and stone fruit production in the United States. *Pest management science*, **67**, 1368-
601 1374. <https://doi.org/10.1002/ps.2280>

602 De Bon H, Faye F, Pages J (1997) Development of vegetable cropping systems in the Niayes zone of Senegal.
603 *Experimental Agriculture*, **33**, 83–90. <https://doi.org/10.1017/S0014479797000197>

604 Deguine JP, Aubertot JN, Flor RJ, Lescourret F, Wyckhuys KAG, Ratnadass A (2021) Integrated pest
605 management: good intentions, hard realities. A review. *Agronomy for Sustainable Development*, **41**, 38.
606 <https://doi.org/10.1007/s13593-021-00689-w>

607 Deguine JP, Aubertot JN, Bellon S, Côte F, Lauri PE, Lescourret F, Ratnadass A, Scopel E, Andrieu N, Bàrberi P,
608 Becker N, Bouyer J, Brevault T, Cerdan C, Cortesero AM, Dangles O, Debatte H, Dinh P, Dreyer H,
609 Lamichhane JR (2023) Agroecological crop protection for sustainable agriculture. *Advances in*
610 *agronomy*, **178**, 1-59. <https://doi.org/10.1016/bs.agron.2022.11.002>

611 de Valpine P, Turek D, Paciorek CJ, Anderson-Bergman C, Lang DT, Bodik R (2017) Programming With Models:
612 Writing Statistical Algorithms for General Model Structures With NIMBLE. *Journal of Computational and*
613 *Graphical Statistics*, **26**, 403–413. <https://doi.org/10.1080/10618600.2016.1172487>

614 Diallo I, Ndiaye A, Faye E, Faye M, Sembene M (2021) Does landscape factors drive the genetic diversity and
615 structure of populations of fruit flies, Senegal? Exploratory study of the case of *Bactrocera dorsalis*
616 (Hendel, 1912) in the Niayes, Senegal. *Journal of Entomology and Zoology Studies*, **9**, 47–52.
617 <https://doi.org/10.22271/j.ento.2021.v9.i6a.8883>

618 Diame L, Blatrix R, Grechi I, Rey J-Y, Sane CAB, Vayssières J-F, De Bon H, Diarra K (2015) Relations between the
619 design and management of Senegalese orchards and ant diversity and community composition.
620 *Agriculture, Ecosystems & Environment*, **212**, 94–105. <https://doi.org/10.1016/j.agee.2015.07.004>

621 Diatta P, Rey J-Y, Vayssières J-F, Diarra K, Coly EV, Lechaudel M, Grechi I, Ndiaye S, Ndiaye O (2013) Fruit
622 phenology of citrus, mangoes and papayas influences egg-laying preferences of *Bactrocera invadens*
623 (Diptera: Tephritidae). *Fruits*, **68**, 507–516. <https://doi.org/10.1051/fruits/2013093>

624 Diatta P (2016) Relations entre la typologie des agro-écosystèmes fruitiers et les fluctuations de la population
625 de la mouche des fruits : *Bactrocera dorsalis* (Hendel) dans les régions de Dakar et Thiès (Sénégal). *PhD*
626 *Thesis, Cheikh Anta Diop University*.

627 Didan K (2015) MOD13Q1 MODIS/Terra vegetation indices 16-day L3 global 250m SIN grid V006 [Data set].
628 *NASA eosdis land processes daac*, **10**, 415. <https://doi.org/10.5067/MODIS/MOD13Q1.006>

629 Didan K, Munoz AB, Solano R, Huete A (2015) MODIS vegetation index user's guide (MOD13 series). *University*
630 *of Arizona: Vegetation Index and Phenology Lab*, **35**, 2–33.

631 Dieng EO, Ndiaye S, Faye PD, Balayara A, Badji K, Sembene PM (2019) New inventory of the diversity and
632 seasonal abundance of Tephritid fruit fly species on mango orchards in Senegal. *Journal of Entomology*
633 *and Zoology Studies*, **7**, 975-986.

634 Diouf EG, Brévault T, Ndiaye S, Faye E, Chailleux A, Diatta P, Piou C (2022) An agent-based model to simulate
635 the boosted Sterile Insect Technique for fruit fly management. *Ecological Modelling*, **468**, 109951.
636 <https://doi.org/10.1016/j.ecolmodel.2022.109951>

637 Dongmo MAK, Fiaboe KKM, Kekeunou S, Nanga SN, Kuate AF, Tonnang HEZ, Gnanvossou D, Hanna R (2021)
638 Temperature-based phenology model to predict the development, survival, and reproduction of the
639 oriental fruit fly *Bactrocera dorsalis*. *Journal of Thermal Biology*, **97**, 102877.
640 <https://doi.org/10.1016/j.jtherbio.2021.102877>

641 Drew RAI, Tsuruta K, White IM (2005) A new species of pest fruit fly (Diptera: Tephritidae: Dacinae) from Sri
642 Lanka and Africa. *African entomology*, **13**, 149-154.

643 Dray S, Dufour A-B (2007) The ade4 Package: Implementing the Duality Diagram for Ecologists. *Journal of*
644 *Statistical Software*, **22**, 1–20. <https://doi.org/10.18637/jss.v022.i04>

645 Ekesi S, Billah MK (2006) A Field Guide to the Management of Economically Important Tephritid Fruit Flies in
646 Africa. 2nd edition. *Nairobi, Kenya: icipe Science Press*.

647 Ekesi S, Nderitu PW, Rwomushana I (2006) Field infestation, life history and demographic parameters of the
648 fruit fly *Bactrocera invadens* (Diptera: Tephritidae) in Africa. *Bulletin of Entomological Research*, **96**, 379-
649 386. <https://doi.org/10.1079/BER2006442>

650 Ekesi S, Chabi-Olaye A, Subramanian S, Borgemeister C (2011) Horticultural pest management and the African
651 economy: successes, challenges and opportunities in a changing global environment. *Acta*
652 *Horticulturae*, **911**, 165-183. <https://doi.org/10.17660/ActaHortic.2011.911.17>

653 Elith J, Leathwick JR, Hastie T (2008) A working guide to boosted regression trees. *Journal of animal ecology*,
654 **77**, 802–813. <https://doi.org/10.1111/j.1365-2656.2008.01390.x>

655 Epsky ND, Kendra PE, Schnell EQ (2014) History and development of food-based attractants. In: *Trapping and*
656 *the detection, control, and regulation of tephritid fruit flies: lures, area-wide programs, and trade*
657 *implications*, 75-118, Springer Netherlands, Dordrecht. <https://doi.org/10.1007/978-94-017-9193-9>

658 Faye M, Ndiaye A, Diallo I, Sembene PM (2021) Genetic identification of populations of *Bactrocera dorsalis*
659 (Diptera Tephritidae) in the Niayes and Lower Casamance areas in Senegal. *Journal of Applied*
660 *Biosciences*, **158**, 16351–16362. <https://doi.org/10.35759/JABs.158.9>

661 Froerer KM, Peck SL, McQuate GT, Vargas RI, Jang EB, McInnis DO (2010) Long-Distance Movement of
662 *Bactrocera dorsalis* (Diptera: Tephritidae) in Puna, Hawaii: How far can they go? *American Entomologist*,
663 **56**, 88–95. <https://doi.org/10.1093/ae/56.2.88>

664 Gao B-C (1996) NDWI—A normalized difference water index for remote sensing of vegetation liquid water
665 from space. *Remote Sensing of Environment*, **58**, 257–266. [https://doi.org/10.1016/S0034-4257\(96\)00067-3](https://doi.org/10.1016/S0034-4257(96)00067-3)

666

667 Grechi I, Sane CAB, Diame L, De Bon H, Benneveau A, Michels T, Huguenin V, Malezieux E, Diarra K, Rey J-Y
668 (2013) Mango-based orchards in Senegal: diversity of design and management patterns. *Fruits*, **68**, 447–
669 466. <https://doi.org/10.1051/fruits/2013094>

670 Grinsztajn L, Oyallo E, Varoquaux G (2022) Why do tree-based models still outperform deep learning on
671 typical tabular data? *Advances in Neural Information Processing Systems*, **35**, 507-520.

672 Gu Y, Brown JF, Verdin JP, Wardlow B (2007) A five-year analysis of MODIS NDVI and NDWI for grassland
673 drought assessment over the central Great Plains of the United States. *Geophysical research letters*, **34**,
674 <https://doi.org/10.1029/2006GL029127>

675 Hochachka WM, Caruana R, Fink D, Munson A, Riedewald M, Sorokina D, Kelling S (2007) Data-Mining
676 Discovery of Pattern and Process in Ecological Systems. *Journal of Wildlife Management*, **71**, 2427-2437.
677 <https://doi.org/10.2193/2006-503>

678 Hong SC, Magarey R, Borchert DM, Vargas RI, Souder S (2015) Site-specific temporal and spatial validation of
679 a generic plant pest forecast system with observations of *Bactrocera dorsalis* (oriental fruit fly).
680 *NeoBiota*, **27**, 37–67. <https://doi.org/10.3897/neobiota.27.5177>

681 Hou B, Xie Q, Zhang R (2006) Depth of pupation and survival of the Oriental fruit fly, *Bactrocera dorsalis*
682 (Diptera: Tephritidae) pupae at selected soil moistures. *Applied Entomology and Zoology*, **41**, 515–520.
683 <https://doi.org/10.1303/aez.2006.515>

684 Ibrahim EA, Salifu D, Mwalili S, Dubois T, Collins R, Tonnang HEZ (2022) An expert system for insect pest
685 population dynamics prediction. *Computers and Electronics in Agriculture*, **198**, 107124.
686 <https://doi.org/10.1016/j.compag.2022.107124>

687 Inskeep JR, Allen AP, Taylor PW, Rempoulakis P, Weldon CW (2021) Canopy distribution and microclimate
688 preferences of sterile and wild Queensland fruit flies. *Scientific Reports*, **11**, 13010.
689 <https://doi.org/10.1038/s41598-021-92218-8>

690 Jackson CG, Long JP, Klungness LM (1998) Depth of Pupation in Four Species of Fruit Flies (Diptera:
691 Tephritidae) in Sand With and Without Moisture. *Journal of Economic Entomology*, **91**, 138–142.
692 <https://doi.org/10.1093/jee/91.1.138>

693 Jolivot A (2021) Cartographie de l'occupation du sol de la zone des Niayes (Sénégal) en 2018 (1.5 m de
694 résolution) V1 [Data set]. *CIRAD Dataverse*. <https://doi.org/10.18167/DVN1/KJAS6S>

695 Johnson R, Zhang T (2013) Learning nonlinear functions using regularized greedy forest. *IEEE transactions on*
696 *pattern analysis and machine intelligence*, **36**, 942-954. <https://doi.org/10.1109/TPAMI.2013.159>

697 Karger DN, Conrad O, Böhrner J, Kawohl T, Kreft H, Soria-Auza RW, Zimmermann NE, Linder HP, Kessler M
698 (2017) Climatologies at high resolution for the earth's land surface areas. *Scientific Data*, **4**, 170122.
699 <https://doi.org/10.1038/sdata.2017.122>

700 Karger DN, Conrad O, Böhrner J, Kawohl T, Kreft H, Soria-Auza RW, Zimmermann NE, Linder HP, Kessler M
701 (2021) Climatologies at high resolution for the earth's land surface areas. *EnviDat*.
702 <https://doi.org/10.16904/envidat.228>.

703 Kennedy GG, Storer NP (2000) Life Systems of Polyphagous Arthropod Pests in Temporally Unstable Cropping
704 Systems. *Annual Review of Entomology*, **45**, 467–493. <https://doi.org/10.1146/annurev.ento.45.1.467>

705 Kelling S, Hochachka WM, Fink D, Riedewald M, Caruana R, Ballard G, Hooker G (2009) Data-intensive Science:
706 A New Paradigm for Biodiversity Studies. *BioScience*, **59**, 613–620.
707 <https://doi.org/10.1525/bio.2009.59.7.12>

708 Konta IS, Djiba S, Sane S, Diassi L, Ndiaye AB, Noba K (2015) Etude de la dynamique de *Bactrocera dorsalis*
709 (Hendel) (Diptera: Tephritidae) dans les vergers de mangues en Basse Casamance : influence des
710 facteurs climatiques. *International Journal of Biological and Chemical Sciences*, **9**, 2698–2715.
711 <https://doi.org/10.4314/ijbcs.v9i6.15>

712 Liu J, Xiong X, Pan Y, Yang L, Li X (2011) Research progress of *Bactrocera dorsalis* and its species
713 complex. *Agricultural Science & Technology-Hunan*, **12**, 1657-1661.

714 Liu Y, Just A (2021). SHAPforxgboost: SHAP Plots for 'XGBoost'. *R package version 0.1.1*. [https://CRAN.R-](https://CRAN.R-project.org/package=SHAPforxgboost)
715 [project.org/package=SHAPforxgboost](https://CRAN.R-project.org/package=SHAPforxgboost)

716 Louzeiro LRF, Souza-Filho MFD, Raga A, Gislotti LJ (2021) Incidence of frugivorous flies (Tephritidae and
717 Lonchaeidae), fruit losses and the dispersal of flies through the transportation of fresh fruit. *Journal of*
718 *Asia-Pacific Entomology*, **24**, 50–60. <https://doi.org/10.1016/j.aspen.2020.11.006>

719 Lundberg SM, Lee S-I (2017) A unified approach to interpreting model predictions. *Advances in neural*
720 *information processing systems*, **30**, 4765-4774.

721 Lundberg SM, Erion GG, Lee S-I (2018) Consistent individualized feature attribution for tree ensembles. *arXiv*
722 *preprint arXiv:1802.03888*.

723 MacArthur RH (1957) On the relative abundance of bird species. *Proceedings of the National Academy of*
724 *Sciences*, **43**, 293–295. <https://doi.org/10.1073/pnas.43.3.293>

725 Makumbe LD, Moropa TP, Manrakhan A, Weldon CW (2020) Effect of sex, age and morphological traits on
726 tethered flight of *Bactrocera dorsalis* (Hendel) (Diptera: Tephritidae) at different temperatures.
727 *Physiological Entomology*, **45**, 110–119. <https://doi.org/10.1111/phen.12323>

728 Manrakhan A, Daneel JH, Beck R, Virgilio M, Meganck K, De Meyer M (2017) Efficacy of trapping systems for
729 monitoring of Afrotropical fruit flies. *Journal of Applied Entomology*, **141**, 825–840.
730 <https://doi.org/10.1111/jen.12373>

731 Manrakhan A, Daneel JH, Beck R; Virgilio M, Meganck K, De Meyer M (2019) Monitoring of fruit fly pests in
732 commercial citrus orchards: temporal patterns of male and female catches. *South African Fruit Journal*,
733 **19**, 50-52.

734 Motswagole R, Gotcha N, Nyamukondiwa C (2019) Thermal biology and seasonal population abundance of
735 *Bactrocera dorsalis* Hendel (Diptera: Tephritidae): implications on pest management. *International*
736 *Journal of Insect Science*, **11**, 1-9. <https://doi.org/10.1177/1179543319863417>

737 Mutamiswa R, Nyamukondiwa C, Chikowore G, Chidawanyika F (2021) Overview of oriental fruit fly,
738 *Bactrocera dorsalis* (Hendel) (Diptera: Tephritidae) in Africa: From invasion, bio-ecology to sustainable
739 management. *Crop Protection*, **141**, 105492. <https://doi.org/10.1016/j.cropro.2020.105492>

740 Ndiaye M, Dieng EO, Delhove G (2008) Population dynamics and on-farm fruit fly integrated pest management
741 in mango orchards in the natural area of Niayes in Senegal. *Pest Management in Horticultural*
742 *Ecosystems*, **14**, 1- 8.

743 Ndiaye O (2009) Plantes hôtes et foyers de réinfestation des mouches des fruits : facteurs phénologiques,
744 morpho physiologiques déterminants sur les infestations de la mangue. *M. Sc. Degree, Thiès University.*

745 Ndiaye O, Vayssieres J-F, Rey J-Y, Ndiaye S, Diedhiou PM, Ba CT, Diatta P (2012) Seasonality and range of fruit
746 fly (Diptera: Tephritidae) host plants in orchards in Niayes and the Thiès Plateau (Senegal). *Fruits*, **67**,
747 311–331. <https://doi.org/10.1051/fruits/2012024>

748 Nielsen D (2016) Tree boosting with xgboost-why does xgboost win" every" machine learning competition?
749 Master thesis. NTNU.

750 Papaix J, Soubeyrand S, Bonnefon O, Walker E, Louvrier J, Klein E, Roques L (2022) Inferring Mechanistic
751 Models in Spatial Ecology Using a Mechanistic-Statistical Approach. In: *Statistical Approaches for Hidden*
752 *Variables in Ecology* , 69–95. John Wiley & Sons, Ltd. <https://doi.org/10.1002/9781119902799.ch4>

753 Rosenheim JA, Parsa S, Forbes AA, Krimmel WA, Law YH, Segoli M, Segoli M, Sivakoff FS, Zaviezo T, Gross K
754 (2011) Ecoinformatics for Integrated Pest Management: Expanding the Applied Insect Ecologist’s Tool-
755 Kit. *Journal of Economic Entomology*, **104**, 331–342. <https://doi.org/10.1603/EC10380>

756 Rosenheim JA, Meisner MH (2013) Ecoinformatics can reveal yield gaps associated with crop-pest
757 interactions: a proof-of-concept. *PLoS One*, **8**, e80518. <https://doi.org/10.1371/journal.pone.0080518>

758 Rosenheim JA, Gratton C (2017) Ecoinformatics (Big Data) for Agricultural Entomology: Pitfalls, Progress, and
759 Promise. *Annual Review of Entomology*, **62**, 399–417. [https://doi.org/10.1146/annurev-ento-031616-
760 035444](https://doi.org/10.1146/annurev-ento-031616-035444)

761 Rosset S, Zhu J, Hastie T (2004) Boosting as a regularized path to a maximum margin classifier. *The Journal of*
762 *Machine Learning Research*, **5**, 941-973. <https://dl.acm.org/doi/10.5555/1005332.1016790>

763 Rossi-Stacconi MV, Kaur R, Mazzoni V, Ometto L, Grassi A, Gottardello A, Rota-Stabelli O, Anfora G (2016)
764 Multiple lines of evidence for reproductive winter diapause in the invasive pest *Drosophila suzukii*:
765 useful clues for control strategies. *Journal of Pest Science*, **89**, 689–700.
766 <https://doi.org/10.1007/s10340-016-0753-8>

767 Rwomushana I, Ekesi S, Ogol CKPO, Gordon I (2008) Effect of temperature on development and survival of
768 immature stages of *Bactrocera invadens* (Diptera: Tephritidae). *Journal of Applied Entomology*, **132**,
769 832–839. <https://doi.org/10.1111/j.1439-0418.2008.01318.x>

770 Serit M, Tan K-H (1990) Immature life table of a natural population of *Dacus dorsalis* in a village ecosystem.
771 *Tropical Pest Management*, **36**, 305–309. <https://doi.org/10.1080/09670879009371493>

772 Sigrist F (2022) Gaussian process boosting. *The Journal of Machine Learning Research*, **23**, 10565-10610

773 Sigrist F (2023) gpboost: Combining Tree-Boosting with Gaussian Process and Mixed Effects Models. *R*
774 *package version 1.2.3*. <https://CRAN.R-project.org/package=gpboost>

775 Soulsby RL, Thomas JA (2012) Insect population curves: modelling and application to butterfly transect data.
776 *Methods in Ecology and Evolution*, **3**, 832–841. <https://doi.org/10.1111/j.2041-210X.2012.00227.x>

- 777 Stack Whitney K, Meehan TD, Kucharik CJ, Zhu J, Townsend PA, Hamilton K, Gratton C (2016) Explicit modeling
778 of abiotic and landscape factors reveals precipitation and forests associated with aphid abundance.
779 *Ecological Applications*, **26**, 2600–2610. <https://doi.org/10.1002/eap.1418>
- 780 Susanto A, Faradilla MG, Sumekar Y, Yudistira DH, Murdita W, Permana AD, Djaya L, Subakti Putri SN (2022)
781 Effect of various depths of pupation on adult emergence of interspecific hybrid of *Bactrocera*
782 *carambolae* and *Bactrocera dorsalis*. *Scientific Reports*, **12**, 4235. [https://doi.org/10.1038/s41598-022-](https://doi.org/10.1038/s41598-022-08295-w)
783 [08295-w](https://doi.org/10.1038/s41598-022-08295-w)
- 784 Thorat L, Nath BB (2018) Insects With Survival Kits for Desiccation Tolerance Under Extreme Water Deficits.
785 *Frontiers in Physiology*, **9**. <https://doi.org/10.3389/fphys.2018.01843>
- 786 Vargas RI, Walsh WA, Jang EB, Armstrong JW, Kanehisa DT (1996) Survival and Development of Immature
787 Stages of Four Hawaiian Fruit Flies (Diptera: Tephritidae) Reared at Five Constant Temperatures. *Annals*
788 *of the Entomological Society of America*, **89**, 64–69. <https://doi.org/10.1093/aesa/89.1.64>
- 789 Vargas RI, Walsh WA, Kanehisa D, Jang EB, Armstrong JW (1997) Demography of Four Hawaiian Fruit Flies
790 (Diptera: Tephritidae) Reared at Five Constant Temperatures. *Annals of the Entomological Society of*
791 *America*, **90**, 162–168. <https://doi.org/10.1093/aesa/90.2.162>
- 792 Vargas RI, Piñero JC, Miller NW (2018) Effect of physiological state on female Melon fly (Diptera: Tephritidae)
793 attraction to host and food odor in the field. *Journal of economic entomology*, **111**, 1318-1322.
794 <https://doi.org/10.1093/jee/toy092>
- 795 Vayssières J-F, Korie S, Coulibaly O, Temple L, Boueyi SP (2008) The mango tree in central and northern Benin:
796 cultivar inventory, yield assessment, infested stages and loss due to fruit flies (Diptera Tephritidae).
797 *Fruits*, **63**, 335–348. <https://doi.org/10.1051/fruits:2008035>
- 798 Vayssières J-F, Korie S, Ayegnon D (2009) Correlation of fruit fly (Diptera Tephritidae) infestation of major
799 mango cultivars in Borgou (Benin) with abiotic and biotic factors and assessment of damage. *Crop*
800 *protection*, **28**, 477–488. <https://doi.org/10.1016/j.cropro.2009.01.010>
- 801 Vayssières J-F, Vannière H, Gueye PS, Barry O, Hanne AM, Korie S, Niassy A, Ndiaye Mb, Delhove G (2011)
802 Preliminary inventory of fruit fly species (Diptera, Tephritidae) in mango orchards in the Niayes region,
803 Senegal, in 2004. *Fruits*, **66**, 91–107. <https://doi.org/10.1051/fruits/2011002>
- 804 Vayssières J-F, De Meyer M, Ouagoussounon I, Sinzogan A, Adandonon A, Korie S, Wargui R, Anato F, Hougbo
805 H, Didier C, De Bon H, Goergen G (2015) Seasonal Abundance of Mango Fruit Flies (Diptera: Tephritidae)
806 and Ecological Implications for Their Management in Mango and Cashew Orchards in Benin (Centre &
807 North). *Journal of Economic Entomology*, **108**, 2213–2230. <https://doi.org/10.1093/jee/tov143>
- 808 Vayssières JF, Offenber , Sinzogan A, Adandonon A, Wargui R, Anato F, Hougbo HY, Ouagoussounon I, Diamé
809 L, Quilici S, Rey JY, Goergen G, De Meyer M, Van Mele P (2016) The use of weaver ants in the
810 management of fruit flies in Africa. In: Ekesi, S., Mohamed, S., De Meyer, M. (eds) *Fruit Fly Research and*
811 *Development in Africa - Towards a Sustainable Management Strategy to Improve Horticulture*, 389-434,
812 Springer Verlag. https://doi.org/10.1007/978-3-319-43226-7_18

- 813 Veran S, Simpson SJ, Sword GA, Deveson E, Piry S, Hines JE, Berthier K (2015) Modeling spatio-temporal
814 dynamics of outbreaking species: influence of environment and migration in a locust. *Ecology*, **96**, 737–
815 748. <https://doi.org/10.1890/14-0183.1>
- 816 Veres A, Petit S, Conord C, Lavigne C (2013) Does landscape composition affect pest abundance and their
817 control by natural enemies? A review. *Agriculture, Ecosystems & Environment*, **166**, 110-117.
818 <https://doi.org/10.1016/j.agee.2011.05.027>.
- 819 Wade M, Mignot J, Lazar A, Gaye AT, Carré M (2015) On the spatial coherence of rainfall over the Saloum delta
820 (Senegal) from seasonal to decadal time scales. *Frontiers in Earth Science*, **3**.
821 <https://doi.org/10.3389/feart.2015.00030>
- 822 Wang M, Kornblau SM, Coombes KR (2018) Decomposing the Apoptosis Pathway Into Biologically
823 Interpretable Principal Components. *Cancer Informatics*, **17**.
824 <https://doi.org/10.1177/1176935118771082>
- 825 Wood SN (2017) Generalized Additive Models: An Introduction with R (2nd edition). Chapman and
826 Hall/CRC. Yang P, Carey JR, Dowell RV (1994) Temperature Influences on the Development and
827 Demography of *Bactrocera dorsalis* (Diptera: Tephritidae) in China. *Environmental Entomology*, **23**, 971–
828 974. <https://doi.org/10.1093/ee/23.4.971>

FIGURES

Figure 1 - Summary of the analysis pipeline implemented in this study. All steps presented in the figure are detailed in the section Materials & Methods.

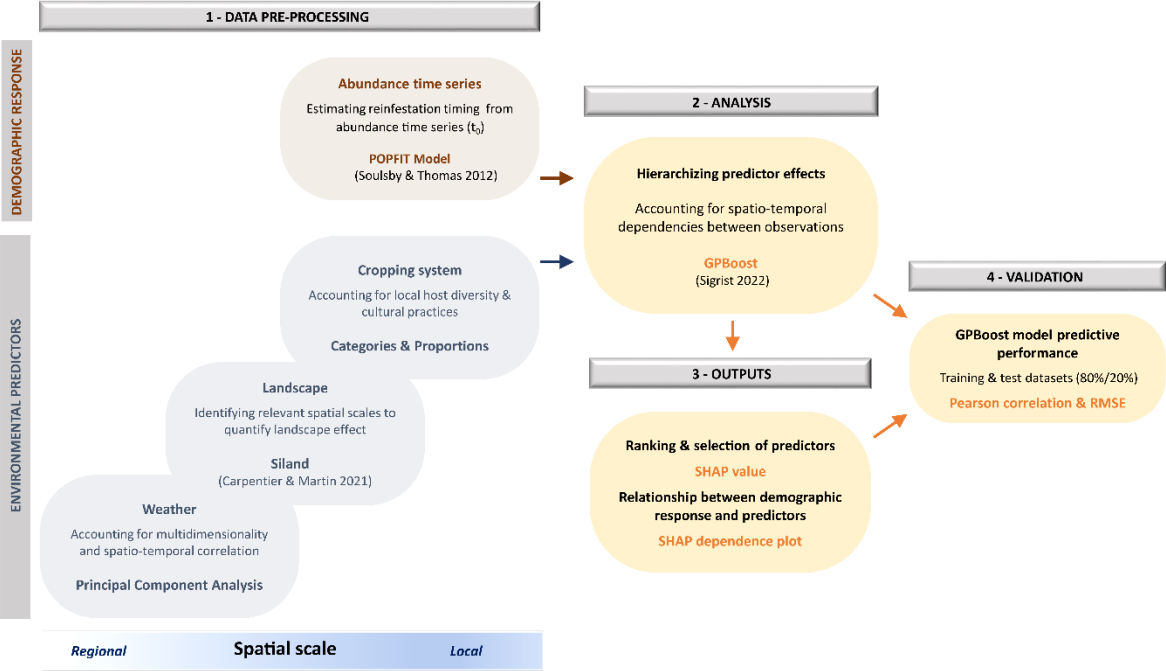


Figure 2 - Study area and sampling sites in the Niayes region, Senegal. The distribution of the 69 orchards monitored for BD abundance among the six main sampling sites (S1 to S6) is 20, 23, 17, 5, 3 and 1, respectively. The background map represents the 13 land use classes (Jolivot 2021) considered in this study.

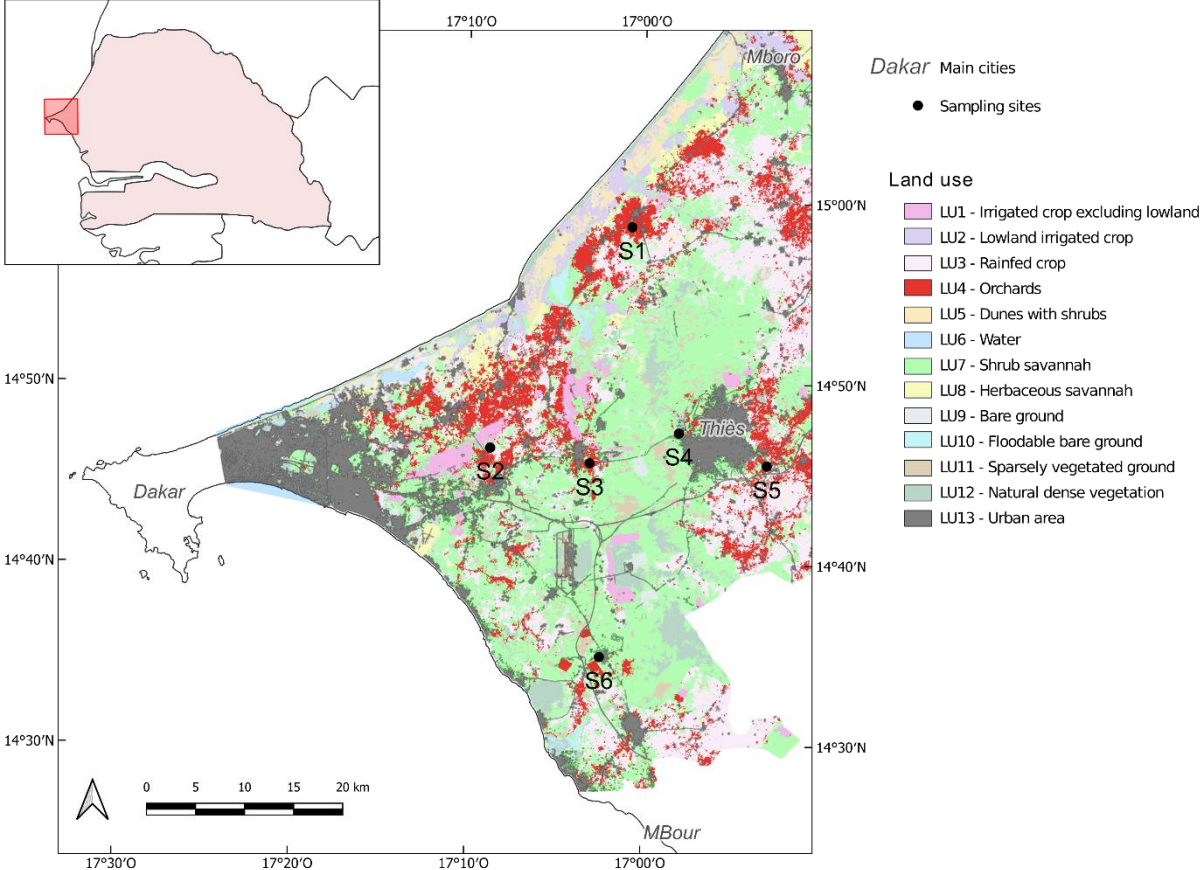


Figure 3 - Illustration of the annual dynamics of BD populations within monitored orchards. The boxplots show the median value (black line), the lower (Q1) and upper (Q3) quartiles (upper and lower box limits), the highest and lowest values excluding outliers (vertical lines, with a maximum length of $1.5 \cdot (Q3 - Q1)$) and outliers (black dots) of the mean number of flies captured per orchard on a weekly basis over the three years of monitoring (2012 to 2014) of the 69 orchards. For a given week, the mean number of captures per orchard is the average of the number of trapped BD in all the traps set in the orchard.

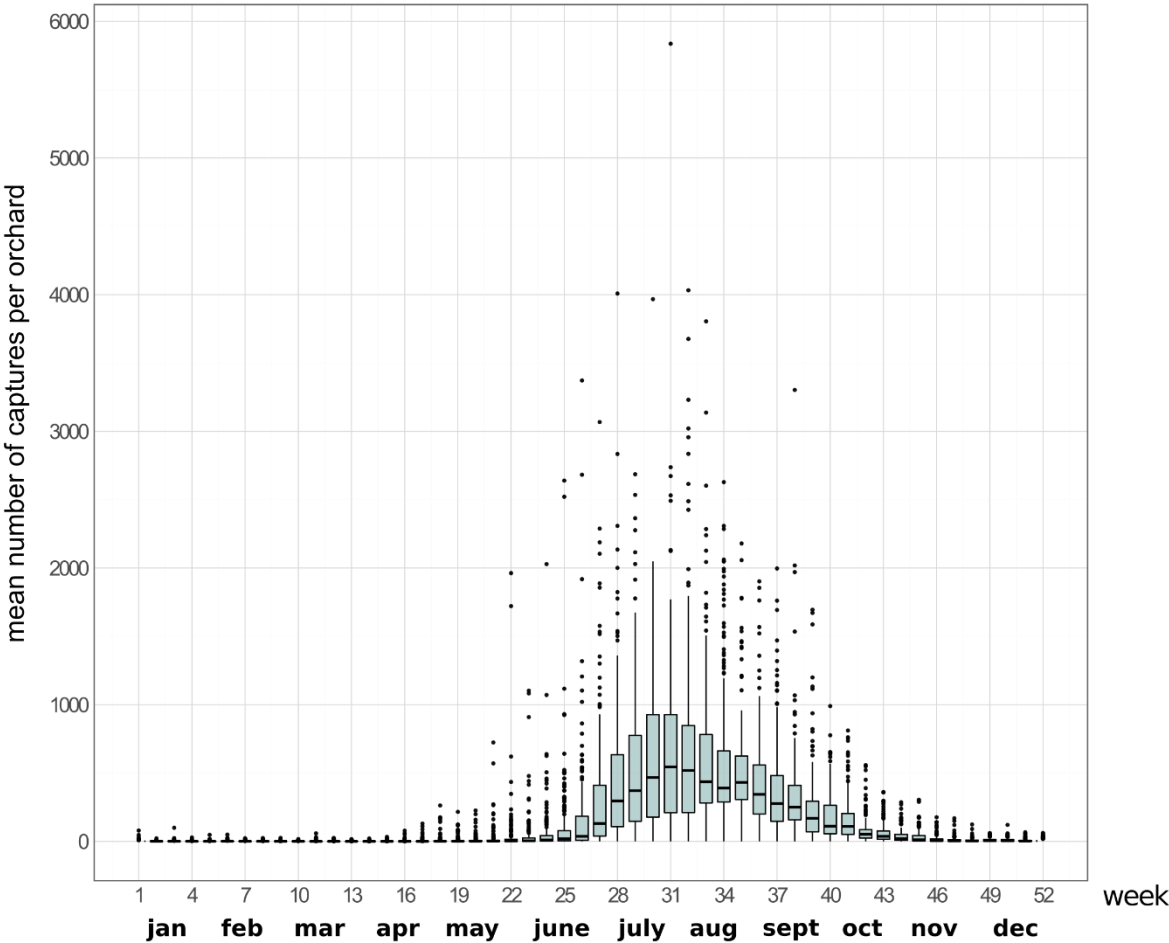


Figure 4 - Ranking of the environmental predictors from the GPBoost model. The ranking is based on the SHAP values resulting from the GPBoost model applied independently on the 500 sample sets: for each predictor, the boxplot shows the median, first quartile, third quartile, lowest and highest values (vertical lines) and outliers (black points) of the S_{mean} values (i.e. the average of individual SHAP values) obtained for the 500 sample sets.

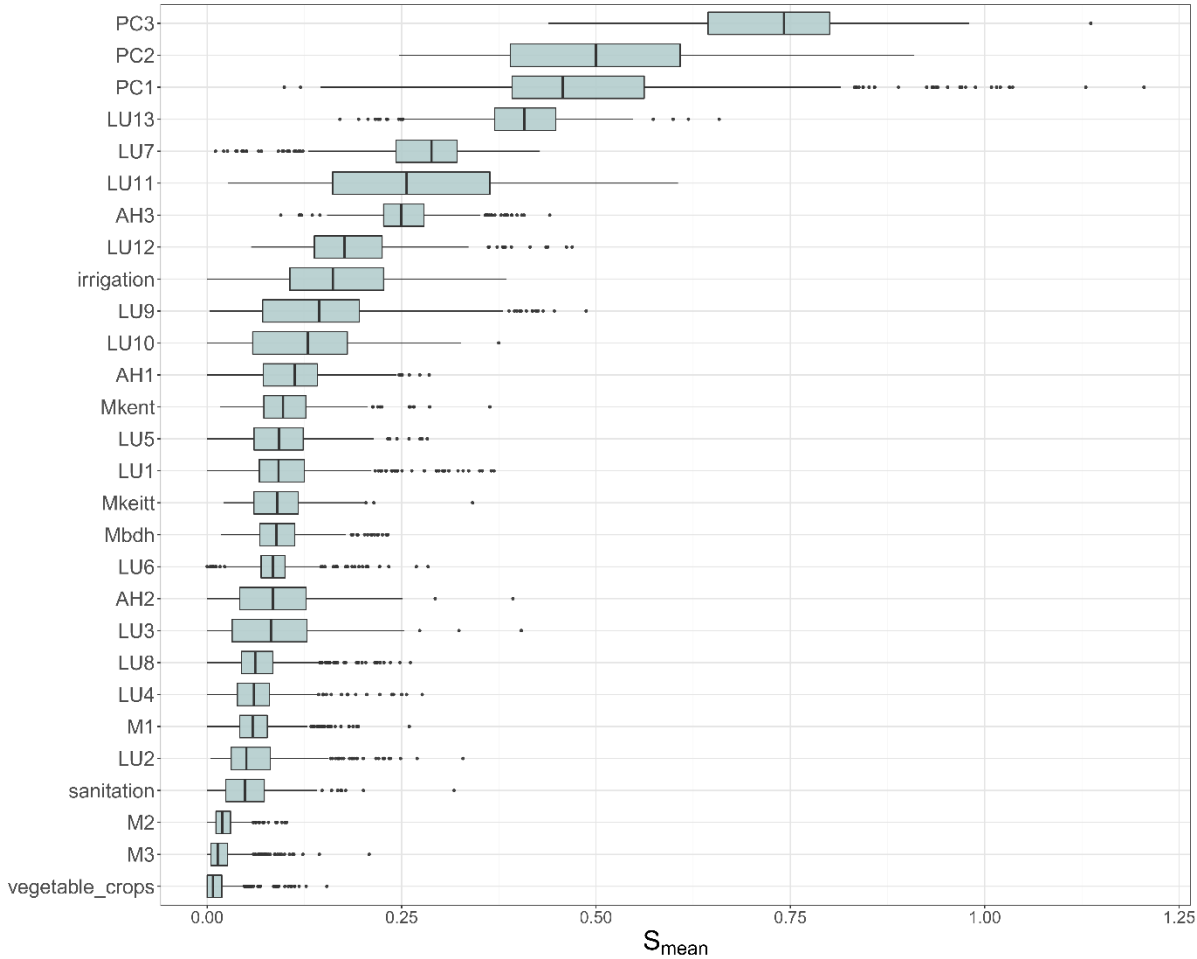
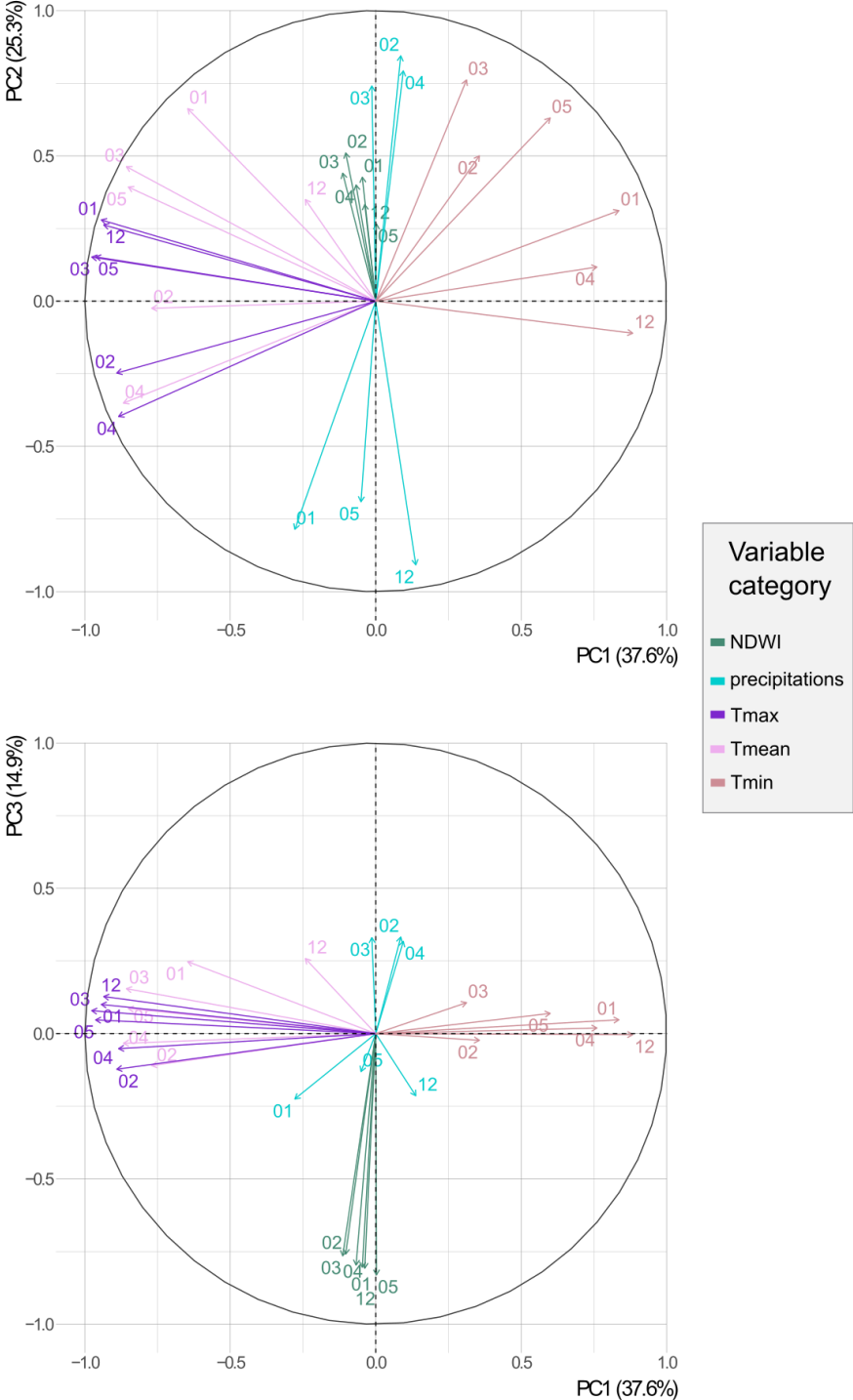


Figure 5 - Results of the PCA performed on the 30 weather and NDWI variables. (A) Variable correlation plots for the first and second PCs (top panel) and first and third PCs (bottom panel): each vector represents a type of input variable (colours) for a given month (numbers) from December (12) to May (05). (B) Maps of the grid cell PCA scores, for each PC and each year of sampling.

(A)



(B)

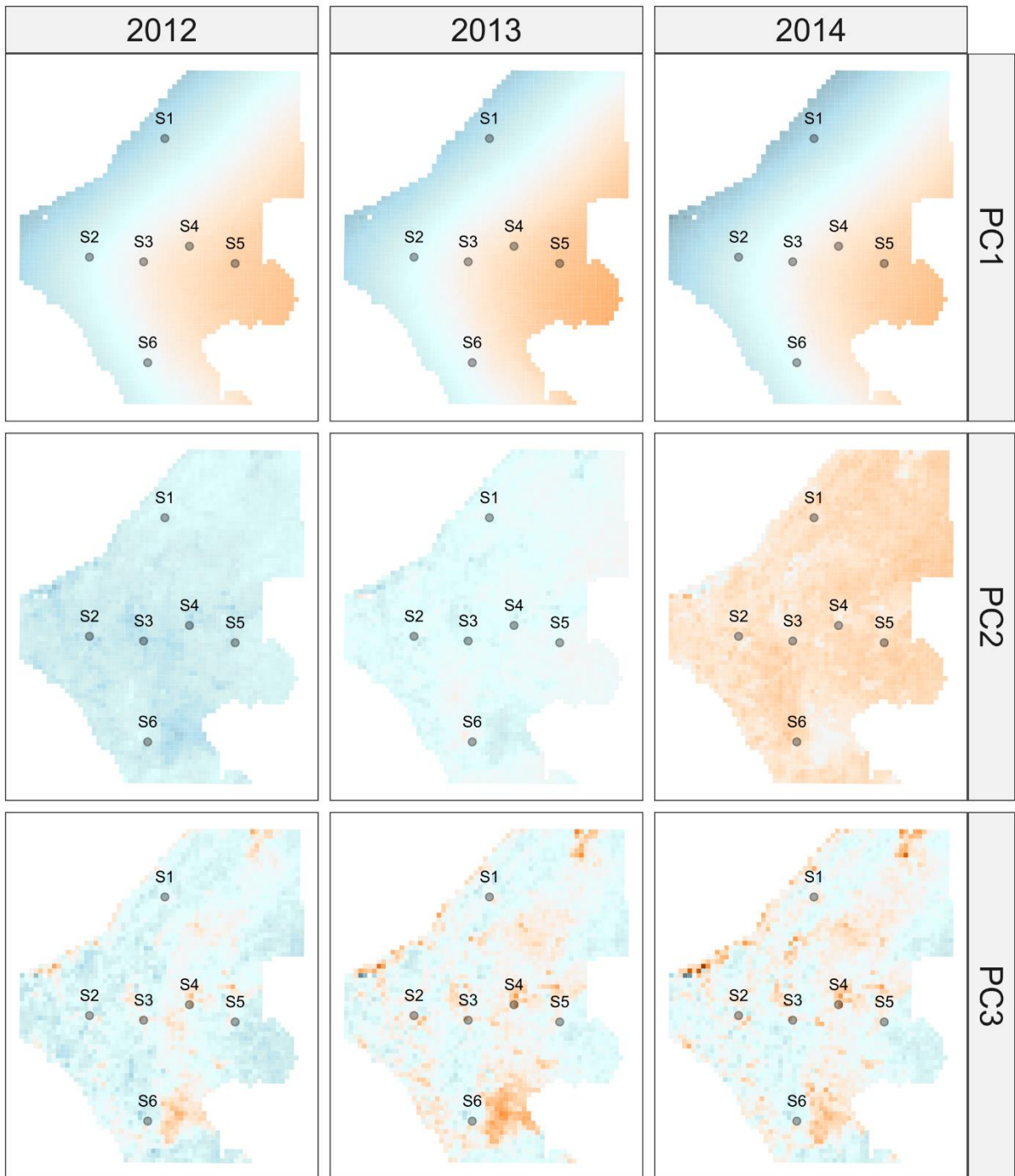


Figure 6 - SHAP dependence plots. For each of the most important environmental predictors in the GPBoost model, the gam-smoothed curve of the SHAP values over the 500 sample sets is represented as a blue line, with its 99% confidence interval in dotted lines and residuals as grey dots. Black lines on the x-axis indicate the distribution of the predictor values. GAM were fitted using thin plate regression splines and by fixing the basis dimension k (ranging from 4 to 9) to avoid overfitting.

